
This is an electronic reprint of the original article.
This reprint may differ from the original in pagination and typographic detail.

Zaremba, Orysia T.; Goldt, Anastasia E.; Khabushev, Eldar M.; Anisimov, Anton S.; Nasibulin, Albert G.

Highly efficient doping of carbon nanotube films with chloroauric acid by dip-coating

Published in:
Materials Science and Engineering B: Solid-State Materials for Advanced Technology

DOI:
[10.1016/j.mseb.2022.115648](https://doi.org/10.1016/j.mseb.2022.115648)

Published: 01/04/2022

Document Version
Publisher's PDF, also known as Version of record

Published under the following license:
CC BY

Please cite the original version:
Zaremba, O. T., Goldt, A. E., Khabushev, E. M., Anisimov, A. S., & Nasibulin, A. G. (2022). Highly efficient doping of carbon nanotube films with chloroauric acid by dip-coating. *Materials Science and Engineering B: Solid-State Materials for Advanced Technology*, 278, Article 115648.
<https://doi.org/10.1016/j.mseb.2022.115648>

This material is protected by copyright and other intellectual property rights, and duplication or sale of all or part of any of the repository collections is not permitted, except that material may be duplicated by you for your research use or educational purposes in electronic or print form. You must obtain permission for any other use. Electronic or print copies may not be offered, whether for sale or otherwise to anyone who is not an authorised user.



Highly efficient doping of carbon nanotube films with chloroauric acid by dip-coating

Orysia T. Zaremba^{a,b}, Anastasia E. Goldt^{a,*}, Eldar M. Khabushev^{a,d}, Anton S. Anisimov^c, Albert G. Nasibulin^{a,d,*}

^a Skolkovo Institute of Science and Technology, 3 Nobel Street, Moscow 121205, Russia

^b Institute of Materials and Systems for Sustainability (IMaSS), Nagoya University, Japan

^c Canatu Ltd. Konalankuja 5, 00390 Helsinki, Finland

^d Aalto University School of Chemical Engineering, Kemistintie 1, 02015, Espoo, Finland

ARTICLE INFO

Keywords:

Dip-coating

Doping

SWCNTs

HAuCl₄

TCFs

In situ sheet resistance measurement

ABSTRACT

Single-walled carbon nanotube (SWCNT) based transparent and conductive films (TCFs) are one of the most prospective materials for novel flexible and stretchable electronic devices. Development of reproducible and scalable doping procedure is the key step towards the widespread implementation of SWCNT TCFs. Here, we thoroughly investigate a dip-coating technique for SWCNT doping as a promising approach for the practical manufacturing of SWCNT films with high performance. We examine the effect of dip-coating parameters on optical and electrical properties of the films using HAuCl₄ solution in isopropyl alcohol (IPA) and *in situ* investigate doping effects. This method appeared to easily fine-tune the optoelectronic parameters of SWCNT films and achieve a record sheet resistance value of 36 Ohm/sq. at the 90% transmittance in the middle of visible spectral range by increasing a work function value from 4.8 (for pristine SWCNTs) to 6.0 eV. The proposed approach allows efficient, uniform, and reproducible fabrication of highly conductive and transparent SWCNT films and opens an avenue for precise tailoring of SWCNT Fermi level for optoelectronic devices.

1. Introduction

Transparent conductive films (TCFs) are principal components for next-generation thin, foldable, and stretchable electronic systems such as wearable devices, [1,2,3] touch screens, [4,5] LEDs, [6] OLEDs, [7] solar cells, [8] gas sensors, [9] *etc.* Nowadays, the mostly spread TCF material is indium-tin-oxide (ITO) due to its superior optoelectronic properties and excellent stability at ambient conditions [10,11]. However, limitations of mechanical properties seriously hampers ITO future applications in flexible and stretchable devices [12].

Thin films of single-walled carbon nanotubes (SWCNTs) [13,14,15,16] are promising materials for the ITO replacement and development of novel electronics beyond the existing one based on brittle ceramics. SWCNT films possess remarkable electrical, [17] optical [18] and mechanical properties [19]. Typically, SWCNT thin films can be prepared either from liquid or gas phases. The former approach firstly requires obtaining stable dispersions of nanotubes in a surfactant solution, [20,21,22] and then SWCNT film deposition either by vacuum filtration, [23] printing, [24] spin-, [20] spray-, [25] rod-, [26] dip-

coating, [27] or Langmuir-Blodgett technique [28]. However, the dispersing process deteriorates the resulting properties of SWCNT films, since ultrasonication introduces defects and shortens the nanotubes, while the presence of surfactants increases the contact resistance between the tubes [29,30]. In contrast, an aerosol (floating-catalyst) chemical vapor deposition (CVD) method [31,32] allows dry film fabrication without the intermediate detrimental stages, keeping intrinsic SWCNT properties unaltered that makes the films superior for electronic component fabrication.

During the synthesis, both semiconducting and metallic SWCNTs are simultaneously produced [13]. Therefore, the formed Schottky barriers at the tube-to-tube interfaces significantly degrade the conductivity of SWCNT films [33]. To enhance the electrical performance of the SWCNT films, usually, adsorption doping is applied [14]. As a result, the Fermi level in the SWCNTs is shifted either in the valence or conduction band, which leads to a decrease in the energy barrier between nanotubes and increase in the charge carrier concentration [34]. Among various dopants (HSO₃Cl, [35] HNO₃, [36] NOBF₄, [37] Au- [34], and Ni-salts, [38,39] MoO_x, [40] TFSI, [41] DDQ, [37] F₄TCNQ [42]) applied for

* Corresponding authors at: Skolkovo Institute of Science and Technology, 3 Nobel Street, Moscow 121205, Russia (A. Nasibulin).

E-mail addresses: a.goldt@skoltech.ru (A.E. Goldt), a.nasibulin@skoltech.ru (A.G. Nasibulin).

<https://doi.org/10.1016/j.mseb.2022.115648>

Received 5 May 2021; Received in revised form 20 December 2021; Accepted 3 February 2022

Available online 17 February 2022

0921-5107/© 2022 The Authors. Published by Elsevier B.V. This is an open access article under the CC BY license (<http://creativecommons.org/licenses/by/4.0/>).

the SWCNT doping, HAuCl_4 is the most promising to achieve the lowest sheet resistance [43] with relatively long-term stability [44].

SWCNT films are usually doped by drop-casting [45], spin- [41] or spray-coating [46], in which a dopant is adsorbed on the surface of the nanotubes. Drop-casting is the simplest method; however, it lacks uniformity, scalability, and reproducibility. The spray-coating can be easily scaled-up, but the reproducibility of the dopant layer is a large challenge. The spin-coating method provides precise control over the coating quality and thickness of a dopant layer, however, dopant losses during the processing make this method economically unfavorable.

A dip-coating is an approach for a thin layer deposition onto a substrate surface. Implementation of the dip-coating technique to SWCNT technology has been extensively studied: several research groups utilized it for fabrication of thin CNT films, [13,27,35,47,48,49] CNTs/AgNWs hybrids, [50] or CNT/polymer composites [51] from CNT dispersion. By this technique, SWCNT films with the sheet resistance of 100 Ohm/sq. were deposited from SWCNT/chlorosulfonic acid dispersion [35]. Besides, the dip-coating technique was utilized to functionalize SWCNTs for electrochemical applications [52]. Even though dip-coating was proven to be an effective technique for a thin layer deposition, it has not been yet examined for the doping of SWCNTs.

Here, we have performed the dip-coating technique for uniform and reproducible doping of SWCNT films. We demonstrate that by adjusting the process parameters such as withdrawal speed and dopant concentration, SWCNT films can be efficiently doped. Fine parameter adjustment allowed us to achieve SWCNT films with the record low sheet resistance of 36 Ohm/sq. at the 90% transmittance in the middle of the visible spectral range which corresponds to the Fermi level shift of 1.2 eV. Our study boosts SWCNT-based transparent and conductive film technology and opens an avenue for optoelectronic applications, requiring high conductivity and precise control of the work function.

2. Experimental

2.1. SWCNT film preparation and doping procedure

High-quality SWCNTs with mean diameter of 2.1 nm were synthesized by an aerosol (floating catalyst) chemical vapor deposition method and collected on filter for subsequent dry transfer onto quartz substrates as described elsewhere [53]. For our studies, we used SWCNT films with the transmittance of 80–85% (at a wavelength of 550 nm).

Chloroauric acid ($\text{HAuCl}_4 \cdot 3\text{H}_2\text{O}$ purity 99%, Sigma-Aldrich) was used to HAuCl_4 solutions in isopropyl alcohol (IPA, Sigma-Aldrich) with concentrations of 0.01, 0.1, 1.0, 3.75, 7.5, 15, 30 and 60 mM. Doping procedure was performed using an automated dip-coating system (Apex Instr. Co. Xdip-MV1) at controlled withdrawal speeds of 50, 100, 200, 300, and 400 mm/min and immersion time of 1 min. After withdrawing the SWCNT films from HAuCl_4 solution, samples were dried in air at room temperature for 10 min.

2.2. Sample characterization

Optical properties of SWCNT films were investigated using PerkinElmer LAMBDA 1050 UV-Vis-NIR spectrophotometer in a wide spectral range from 175 to 2750 nm. The quartz substrate with the doped SWCNT films was wiped off from the backside by isopropyl alcohol before the measurements to remove the chloroauric acid.

Thermo Scientific DXRxi Raman imaging microscope and diode-pumped solid-state laser operating at 532 nm was used to study the quality and doping degree of the SWCNTs.

Ultraviolet photoelectron spectroscopy (UPS) measurements were carried out by using Riken Keiki AC-3 photoelectron spectrometer operating in air. The spectra were measured in the energy range of 4.2–6.5 eV with the resolution of 0.05 eV. The spectra were measured 3 times at 5 different points and averaged (Fig. S1a). The work function of pristine SWCNTs is 4.8 eV.

The sheet resistance of the samples was measured by a linear four-probe method using Jandel RM3000 Test Unit that served as a current source and a digital multimeter. The resistance was measured 3 times at 5 different points and averaged (Fig. S1a). For a comparison of the optoelectrical properties of the SWCNT films, we utilized an equivalent sheet resistance at $T = 90\%$ (at 550 nm) calculated according to the following equation: [54]

$$R_{90} = R_s \cdot \frac{A_{550}}{-\log_{10}(0.9)} \quad (1)$$

where A and R_s are the absorbance (at 550 nm) and sheet resistance of the films.

Investigations of the film morphology were carried out by means of FEI Tecnai G2 F20 transmission electron microscope (TEM) at an acceleration voltage of 100 kV. Samples were prepared by immersing gold TEM grids with deposited SWCNT films into HAuCl_4 solutions by dip-coating technique, followed by the subsequent solvent evaporation in air.

During the doping process, we *in situ* monitored the change in the SWCNT film resistance. For that purpose, we sputtered four 100 nm thick gold contacts with a width of 2.0 mm onto a quartz glass with the surface size of $2.0 \times 3.0 \text{ cm}^2$ and thickness of 3 mm, as shown in Fig. S2. Subsequently, four copper wires were attached to the gold contacts using silver epoxy. Then a SWCNT film with a size of $0.8 \times 2 \text{ cm}^2$ was transferred onto the fabricated substrate so that it touches all the four contacts. Finally, the substrate with a deposited SWCNT film was partially dipped into a dopant solution, while keeping the silver epoxy contacts outside. The current was applied to the outer two contacts, while the potential drop was measured between the middle contacts spaced by 8 mm. The initial and final sheet resistance of the SWCNT films were verified by a linear four-probe measurements using Jandel RM3000 tool.

3. Results and discussion

UV-vis-NIR spectroscopy was used to analyze the electronic structure of SWCNT films before and after chemical doping HAuCl_4 . (Fig. 1, Fig. S3). Doping of carbon nanotubes consists of charge transfer between HAuCl_4 and the nanotubes, where the difference in the work function causes electron depletion in the vicinity of Van Hove singularities in semiconducting (S_{11}, S_{22}) and metallic (M_{11}) SWCNTs and concomitant reduction of Au^{3+} to Au^0 [38]. The stepwise change of the dopant concentration from 0.01 to 60 mM results in a gradual change in the SWCNT electronic structure, that is observed by disappearance of absorption peaks corresponding to the optical transition between Van Hove singularities in semiconducting (S_{11}, S_{22}) and metallic (M_{11}) SWCNTs. At a concentration of 3.75 mM and above, the low energy transitions S_{11}, S_{22} and M_{11} fully disappear, while a new peak attributed to intersubband plasmon [55] arises at 1435 nm (Fig. 1).

Meanwhile, due to the doping by 3.75 mM HAuCl_4 , the 3-fold decrease in the sheet resistance (Fig. 2a) and 12 cm^{-1} blue-shift in the Raman G-mode (Fig. 2b) are observed as a result of complete disappearing of the low energy transitions S_{11}, S_{22}, M_{11} . The steady increase in the work function up to 1 eV (Fig. 2c) fits well the evolution of optical absorption peaks associated with the transitions between different levels of Van Hove singularity in SWCNTs (Fig. 3). The consequent growth of the dopant concentration leads to an increase in the Raman shift (Fig. 2b) with a maximum value of 26 cm^{-1} for a 60 mM solution and a work function of 6.07 eV (Fig. 2c). Thus, an increase of a p-type dopant's concentration leads to a shift in the Fermi level downward and the higher work function, accordingly [34]. Although the 60 mM concentration results in the highest shift of the Raman G-mode and work function, the equivalent sheet resistance is not beneficial when compared to a 30 mM solution. Most likely, this can be explained by formation of a thick dopant layer at the highest HAuCl_4 concentration

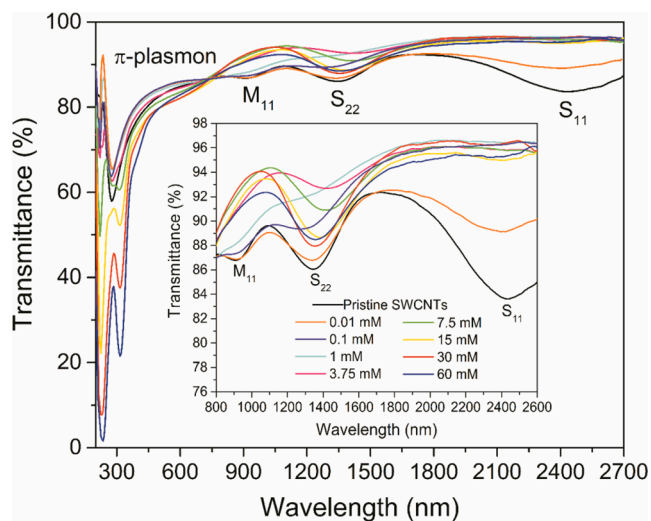


Fig. 1. UV-vis-NIR spectra of SWCNT films doped of different HAuCl₄ concentrations (0.01, 0.1, 1, 3.75, 7.5, 15, 30 and 60 mM). (For interpretation of the references to colour in this figure legend, the reader is referred to the web version of this article).

which lowers the film transmittance in the visible range (Fig. 1). Taking into account that the adsorption doping is associated with a trade-off between conductivity and transmittance, we identified 30 mM HAuCl₄ solution in IPA as an optimal concentration for the highest optoelectronic performance (9-fold decrease in the equivalent sheet resistance and Raman shift of 25 cm⁻¹), which was utilized in our further experiments.

We carried out a control experiment to determine the role of the IPA (Fig. 4a,d) and observed effects in resistance change similar to previously reported by Shu Li *et al.* [56] In the pure solvent, a resistance initially drops due to the bundling process. After 1-minute immersion, an infiltration of IPA molecules results in a gradual increase of the SWCNT film resistance. Over the next 3 h, the equilibrium in the system is practically established. Subsequent withdrawal of the film from IPA leads to a sharp drop in the resistance to the value lower than that of the pristine film as a result of the film densification by surface tension of the solvent during its evaporation. Besides, due to the densification process by IPA, insignificant changes in UV-spectra and Raman G-mode blue-shift are observed (Fig. S4).

In situ measurements of the SWCNT film resistance during the dip-coating revealed slight resistance decrease immediately after the withdrawal of SWCNTs from 1 mM HAuCl₄ solution (Fig. 4b) and a 2-fold resistance drop in the case of 30 mM HAuCl₄ (Fig. 4c). Further solvent evaporation results in resistance decrease due to the film densification. The final trend of the film resistance change strongly depends on the

dopant concentration. It can give either a slight rise at a low concentration (1 mM, Fig. 4b) or a significant drop of the film resistance at high concentrations (30 mM, Fig. 4c).

TEM observation of the films after the doping confirms lower doping capacity of the 1 mM HAuCl₄ solution (Fig. 4b,e) with formation of small-size Au⁰ clusters when compared to the 30 mM HAuCl₄ (Fig. 4c,f).

Previously, it was shown that withdrawal speed is a key factor determining the thickness of the deposited film during a dip-coating process [57]. In fact, there are 3 deposition regimes, so-called: capillary, intermediate, and viscous drag regimes [57]. The capillary regime corresponds to a very low withdrawal speeds (lower than 6 mm/min), resulting in thick film, and it is generally used with non-volatile solvents (e.g. water). In contrast, viscous drag regime (higher than 60 mm/min) is used while working with volatile solvents (e.g. ethanol) and, as a result, intermediate thickness is formed [57]. The intermediate regime associated with both intermixed regimes is implied for ultra-thin films. Dip-coating of SWCNT films in HAuCl₄ solutions was performed with withdrawal speed range of 50–400 mm/min corresponding to both intermediate and viscous drag regimes. To examine the withdrawal speed influence on the doping degree, the immersion time was fixed at one minute.

Our results demonstrate that increasing the withdrawal speed from 50 to 400 mm/min gives additional raise to a doping degree, as can be seen from the intersubband plasmon peak (optical feature observed in highly-doped nanotubes) [55] blue-shift (Fig. 5a) and a gradual increase in Raman G-mode shift from 21 cm⁻¹ to 24 cm⁻¹ (Fig. 5b). At 300 mm/min, the lowest equivalent sheet resistance value of 36 Ohm/sq. is achieved as a result of high doping efficiency. At the maximal withdrawal speed of 400 mm/min, the equivalent sheet resistance increases due to the formation of the thick dopant layer on the nanotubes surface, lowering SWCNT film transmittance.

Long-term resistance measurements of the dip-coated SWCNT films (Fig. 6a,b) show the following trend: the film resistance decreases within 1 min by 60% immediately after the immersion into the dopant solution and then remains constant. After the withdrawal of the film from the solution, the solvent evaporation, accompanied by film densification and additional two-fold resistance decrease takes place. Complete solvent evaporation at ambient conditions occurs during ~ 7 h and subsequently leads to a rise in the film resistance because of the dopant decomposition. Over the following week, the equivalent sheet resistance almost doubles and then practically does not change up to 90 days of monitoring (Fig. 6b).

The optical spectra of the doped SWCNT films highlight the evolution of the film resistance (Fig. 7). Right after the doping, two distinct peaks at 227 and 316 nm from [AuCl₄]⁻ appear [58]. Over time, these two peaks disappear and plasmon peak arising from gold nanoparticles broadens and red-shifts (Fig. 7b). This indicates gold nanoparticle growth as a result of HAuCl₄ decomposition and, as a consequence, gold particle aggregation on the surface of the doped SWCNT film that is

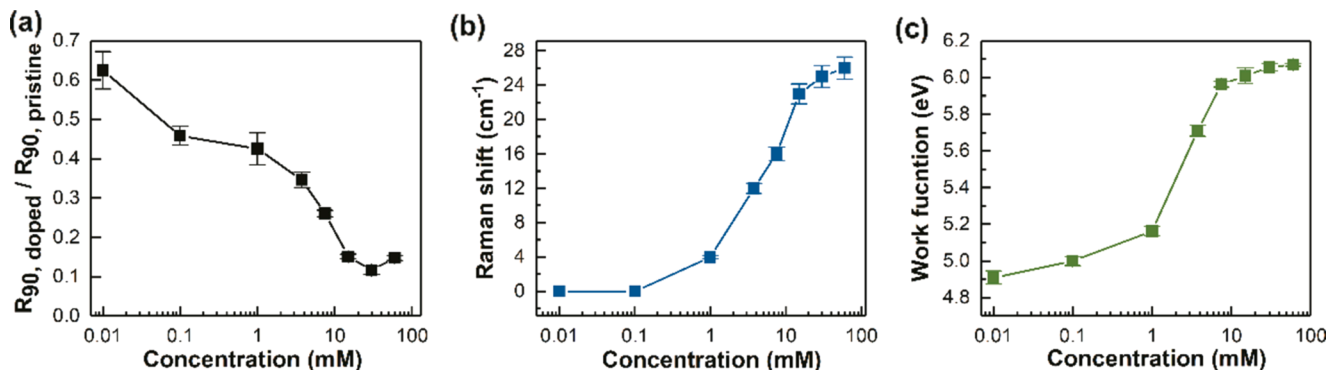


Fig. 2. Dopant concentration (0.01–60 mM HAuCl₄) dependence of (a) equivalent sheet resistance, (b) Raman shift of the G-mode peak, and (c) work function of doped SWCNT films. Withdrawal speed: 300 mm/min, immersion time: 1 min.

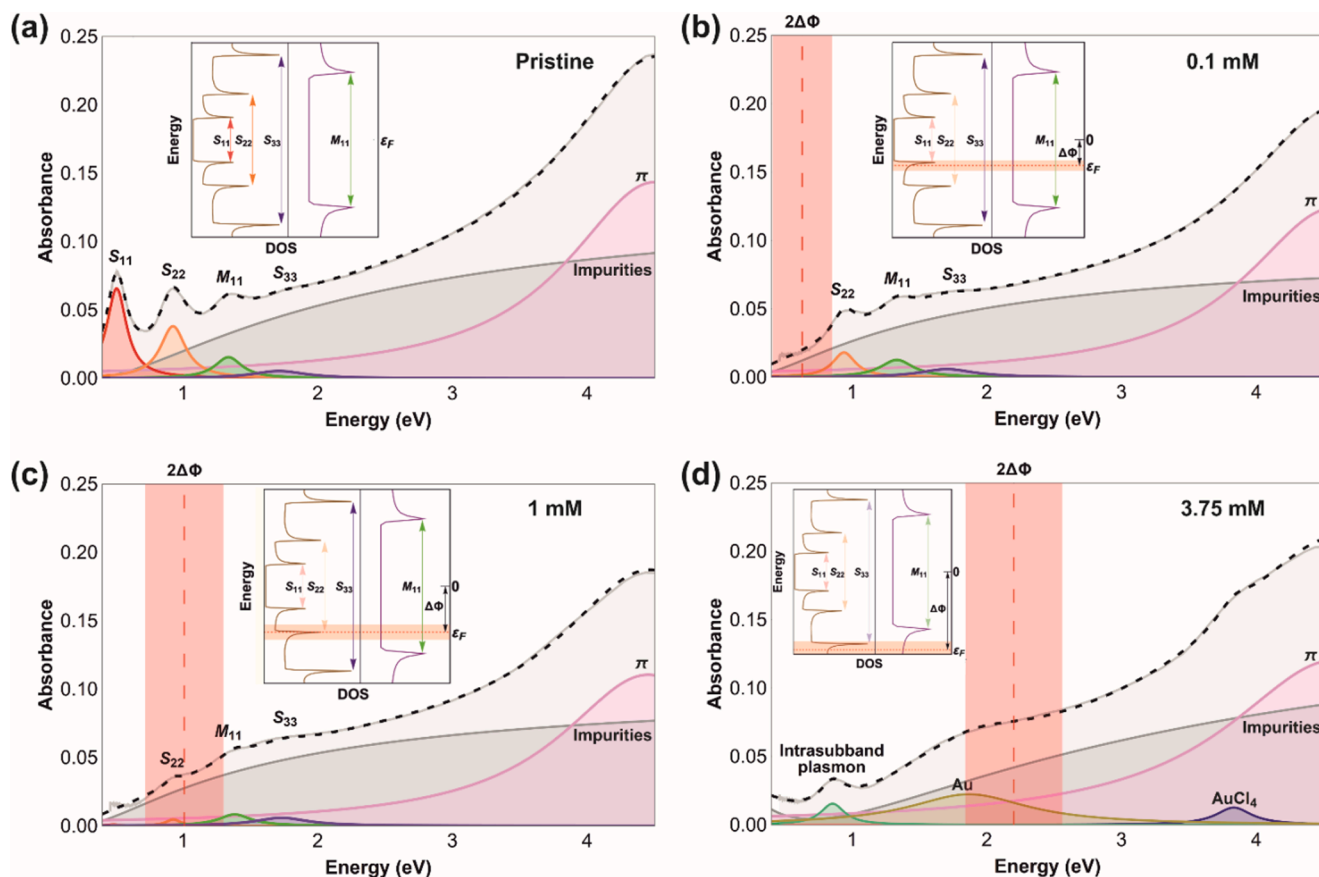


Fig. 3. Evolution of optical absorption peaks attributed to Van Hove singularity after doping with different concentrations of the dopant: (a) pristine SWCNTs, (b) 0.1 mM, (c) 1 mM and (d) 3.75 mM HAuCl₄ solution in IPA.

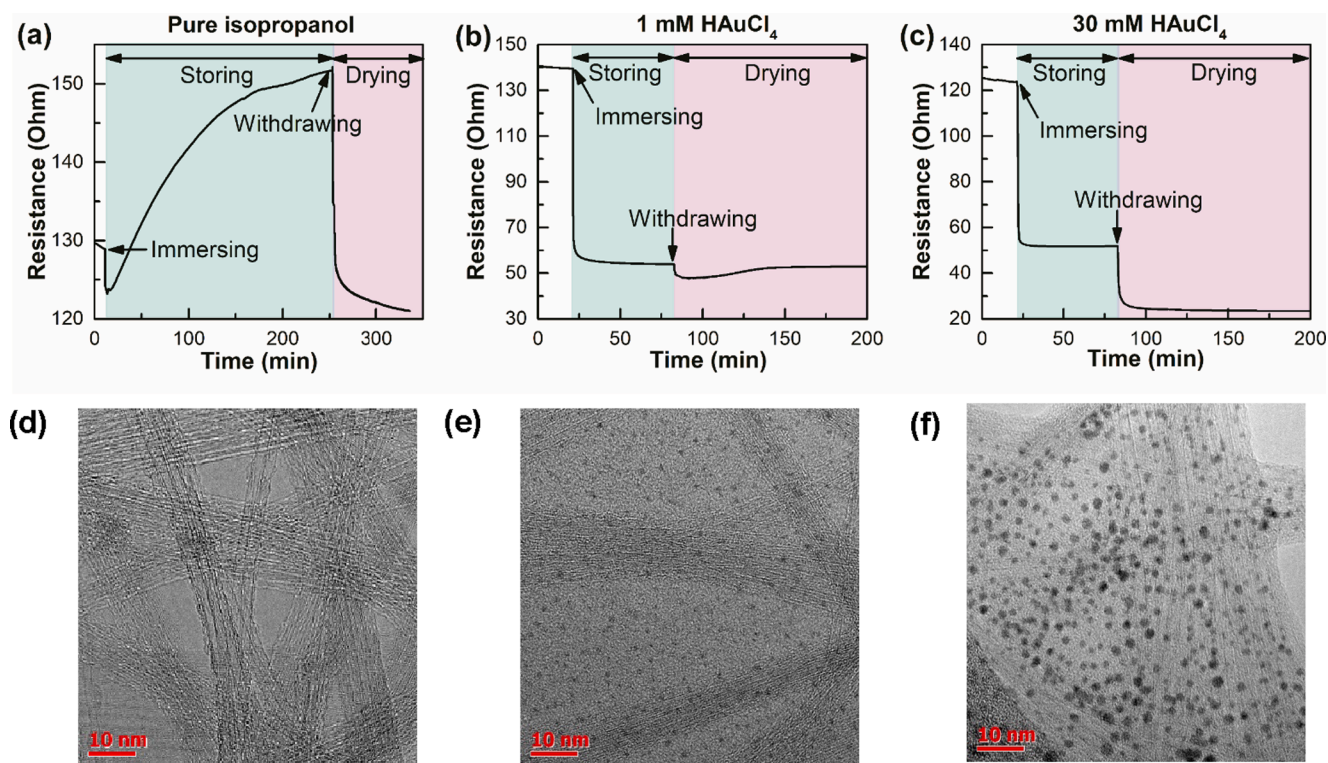


Fig. 4. *In situ* measurements of SWCNT film resistance during dip-coating process in pure (a) IPA, (b) 1 mM and (c) 30 mM HAuCl₄ solution. Typical morphology of SWCNT films (d) after immersing into pure IPA and after the doping in (e) 1 mM and (f) 30 mM HAuCl₄ solution.

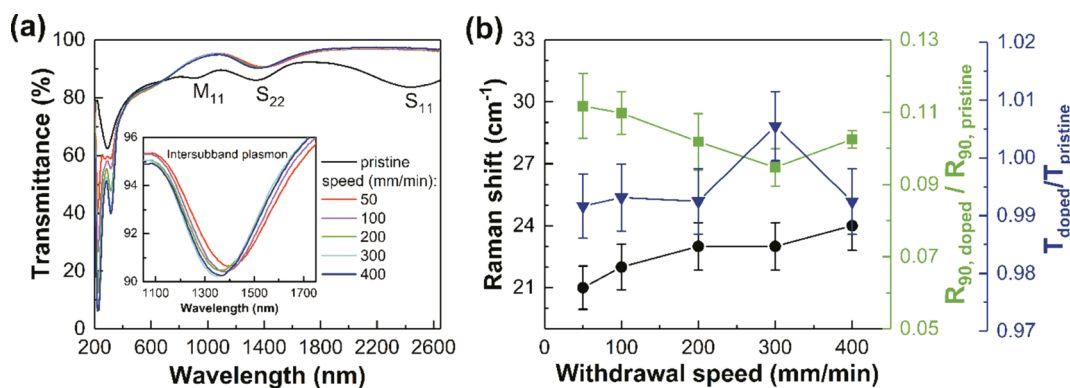


Fig. 5. (a) UV-vis-NIR spectra of HAuCl₄-doped SWCNT films and (b) equivalent sheet resistance, Raman shift and transmittance of SWCNT films doped at different withdrawal speeds (50, 100, 200, 300, 400 mm/min).

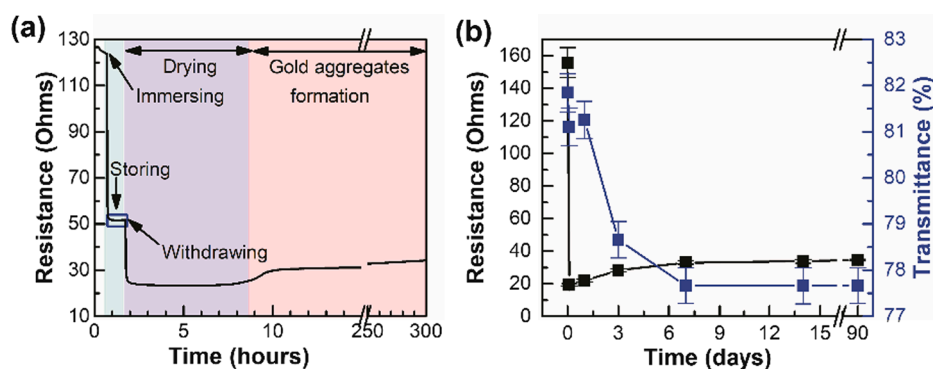


Fig. 6. Time-dependent measurements of (a) the SWCNT film resistance change during and after the dip-coating doping over 12 days; (b) equivalent sheet resistance and transmittance over 90 days.

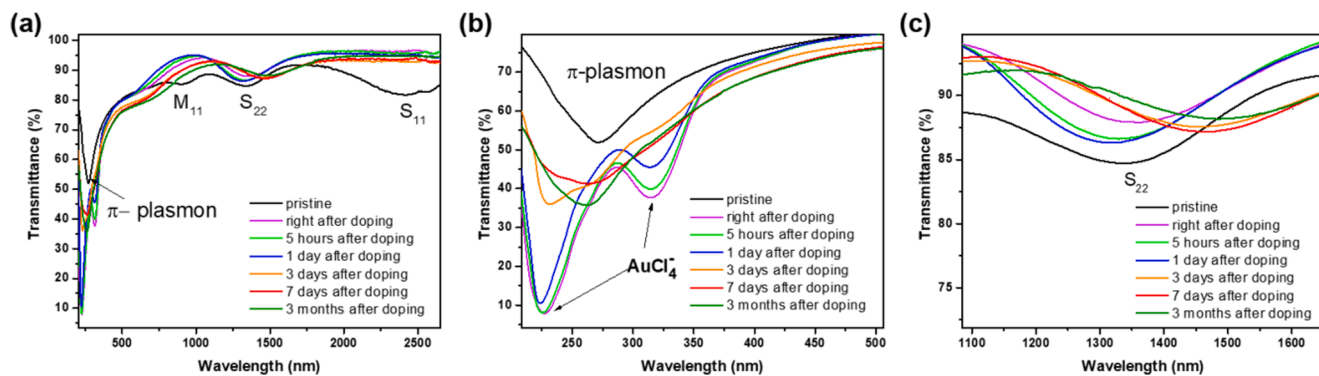


Fig. 7. Time-dependent measurements of UV-vis-NIR spectra of SWCNT film after 30 mM HAuCl₄ doping: (a) survey spectra and evolution of (b) the π -plasmon and (c) the intersubband plasmon regions.

supported by SEM and TEM data (Figure S5).

The evolution of optical absorption after doping is confirmed by position and intensity of intersubband plasmon peak [55] (Fig. 7c). There are two plasmon peaks in SWCNTs. The π -plasmon is a result of collective excitations of the π -band electrons excited by light with parallel polarization to nanotube axis, which is a well-known feature of most graphitic materials. While intersubband plasmon is optical feature observed only in highly-doped nanotube films (usually after the S_{22} transition disappears) in response to the perpendicularly polarized light. It corresponds to electron transition within single conduction (n-type doping) or valence (p-type) band. The calculation of intersubband plasmon dispersion [55] at different Fermi energies (doping levels) reveals that the plasmon energy blue-shifts with Fermi energy rise. The

maximum intersubband plasmon peak intensity is observed on the first day after doping, which may indicate a high doping level; the subsequent red-shifts after one week indicates a decrease in the doping level of SWCNT film, which correlates well with the film resistance trend (Fig. 6b). Since the tetrachloroauric (III) acid has a major contribution to the films' conductivity, "freezing" of the system by creating of a protective layer for the period up to 8 h (Fig. 6a) can preserve the lowest value of the films' resistance.

The uniformity of samples after doping was confirmed by measurements of the sheet resistance, transmittance, and G-peak position in Raman spectra and evaluation of work function in 5 different points (Fig. S1). It was demonstrated that the dip-coating technique allows to obtain fairly uniform distribution of the measured parameters.

The development of the dip-coating doping technique solves the challenge of large-scale transparent and conductive film fabrication. Indeed, the most popular and straightforward doping approaches, such as drop casting, spin-coating, and aerosol coating, primarily lack scalability that makes them incompatible with effective and high-speed roll-to-roll technology. At the same time, the dip-coating procedure could be easily embedded in the continuous roll-to-roll process by immersing roller modules into the reservoir with a dopant.

4. Conclusions

The novel approach for efficient, uniform and reproducible doping of SWCNT films by dip-coating technique was proposed. The electrical and optical properties of the SWCNT films can be controlled by dip-coating's parameters such as the concentration of the dopant solution and the withdrawal speed. Moreover, the influence of the HAuCl_4 concentration in the range from 0.01 to 60 mM on the equivalent sheet resistance of SWCNT films was investigated. Dip-coating into 30 mM HAuCl_4 solution and 300 mm/min withdrawal speed leads to uniformly doped SWCNT films with the state-of-the-art equivalent sheet resistance value of 36 Ω/sq . and high work function value of 6 eV, which corresponds to a Fermi level shift of 1.2 eV. Since the method we utilized is scalable, uniform, reproducible, and compatible with flexible/stretchable substrates, we believe it can become a key technology for fabrication of highly conductive and transparent flexible and stretchable films for future electronic applications.

Declaration of Competing Interest

The authors declare that they have no known competing financial interests or personal relationships that could have appeared to influence the work reported in this paper.

Acknowledgements

We thank Stepan Romanov for *in situ* measurements of SWCNT film resistance during dip-coating process. This work is supported by the Russian Science Foundation (RSF) under grant number 17-19-01787 (dip-coating doping results) and the Ministry of Science and Higher Education of the Russian Federation (project no. FZSR-2020-0007 in the framework of the state assignment no. 075-03-2020-097/1). The authors thank the Council on grants of the President of the Russian Federation grant number HIII-1330.2022.1.3.

Appendix A. Supplementary data

Supplementary data to this article can be found online at <https://doi.org/10.1016/j.mseb.2022.115648>.

References

- [1] C. Wang, K. Xia, H. Wang, X. Liang, Z. Yin, Y. Zhang, Advanced Carbon for Flexible and Wearable Electronics, *Adv. Mater.* 31 (9) (2019) 1801072, <https://doi.org/10.1002/adma.v31.9.10.1002/adma.201801072>.
- [2] H.S. Jo, H.-J. Kwon, T.-G. Kim, C.-W. Park, S. An, A.L. Yarin, S.S. Yoon, Wearable transparent thermal sensors and heaters based on metal-plated fibers and nanowires, *Nanoscale*. 10 (42) (2018) 19825–19834, <https://doi.org/10.1039/C8NR04810J>.
- [3] T. Yamada, Y. Hayamizu, Y. Yamamoto, Y. Yomogida, A. Izadi-Najafabadi, D. N. Futaba, K. Hata, A stretchable carbon nanotube strain sensor for human-motion detection, *Nat. Nanotechnol.* 6 (5) (2011) 296–301, <https://doi.org/10.1038/nnano.2011.36>.
- [4] L. Hu, D.S. Hecht, G. Grüner, Carbon Nanotube Thin Films: Fabrication, Properties, and Applications, *Chem. Rev.* 110 (10) (2010) 5790–5844, <https://doi.org/10.1021/cr9002962>.
- [5] S. Cho, S. Kang, A. Pandya, R. Shanker, Z. Khan, Y. Lee, J. Park, S.L. Craig, H. Ko, Large-Area Cross-Aligned Silver Nanowire Electrodes for Flexible, Transparent, and Force-Sensitive Mechanochromic Touch Screens, *ACS Nano*. 11 (4) (2017) 4346–4357, <https://doi.org/10.1021/acsnano.7b01714>.
- [6] L.u. Li, Z. Yu, W. Hu, C.-H. Chang, Q.i. Chen, Q. Pei, Efficient flexible phosphorescent polymer light-emitting diodes based on silver nanowire-polymer composite electrode, *Adv. Mater.* 23 (46) (2011) 5563–5567, <https://doi.org/10.1002/adma.201103180>.
- [7] J. Gao, X. Mu, X.-Y. Li, W.-Y. Wang, Y. Meng, X.-B. Xu, L.-T. Chen, L.-J. Cui, X. Wu, H.-Z. Geng, Modification of carbon nanotube transparent conducting films for electrodes in organic light-emitting diodes, *Nanotechnology*. 24 (43) (2013) 435201, <https://doi.org/10.1088/0957-4484/24/43/435201>.
- [8] W. Guo, Z. Xu, F. Zhang, S. Xie, H. Xu, X.Y. Liu, Recent Development of Transparent Conducting Oxide-Free Flexible Thin-Film Solar Cells, *Adv. Funct. Mater.* 26 (48) (2016) 8855–8884, <https://doi.org/10.1002/adfm.201603378>.
- [9] S. Bai, C. Sun, P. Wan, C. Wang, R. Luo, Y. Li, J. Liu, X. Sun, Transparent conducting films of hierarchically nanostructured polyaniline networks on flexible substrates for high-performance gas sensors, *Small*. 11 (3) (2015) 306–310, <https://doi.org/10.1002/sml.201401865>.
- [10] U. Betz, M. Kharrazi Olsson, J. Marthy, M.F. Escolá, F. Atamny, Thin films engineering of indium tin oxide: Large area flat panel displays application, *Surf. Coatings Technol.* 200 (20–21) (2006) 5751–5759, <https://doi.org/10.1016/j.surfcoat.2005.08.144>.
- [11] S.K. Park, J.I. Han, W.K. Kim, M.G. Kwak, Deposition of indium-tin-oxide films on polymer substrates for application in plastic-based flat panel displays, *Thin Solid Films*. 397 (1–2) (2001) 49–55, [https://doi.org/10.1016/S0040-6090\(01\)01489-4](https://doi.org/10.1016/S0040-6090(01)01489-4).
- [12] H.S. Jung, K. Eun, Y.T. Kim, E.K. Lee, S.-H. Choa, Experimental and numerical investigation of flexibility of ITO electrode for application in flexible electronic devices, *Microsyst. Technol.* 23 (6) (2017) 1961–1970, <https://doi.org/10.1007/s00542-016-2959-3>.
- [13] LePing Yu, C. Shearer, J. Shapter, Recent Development of Carbon Nanotube Transparent Conductive Films, *Chem. Rev.* 116 (22) (2016) 13413–13453, <https://doi.org/10.1021/acs.chemrev.6b00179>.
- [14] U.N. Maiti, W.J. Lee, J.M. Lee, Y. Oh, J.Y. Kim, J.E. Kim, J. Shim, T.H. Han, S. O. Kim, 25th anniversary article: Chemically modified/doped carbon nanotubes & graphene for optimized nanostructures & nanodevices, *Adv. Mater.* 26 (2014) 40–67, <https://doi.org/10.1002/adma.201303265>.
- [15] Y. Zhou, R. Azumi, Carbon nanotube based transparent conductive films: progress, challenges, and perspectives, *Sci. Technol. Adv. Mater.* 17 (1) (2016) 493–516, <https://doi.org/10.1080/14686996.2016.1214526>.
- [16] S.A. Romanov, A.E. Aliev, B.V. Fine, A.S. Anisimov, A.G. Nasibulin, Highly efficient thermophones based on freestanding single-walled carbon nanotube films, *Nanoscale Horizons*. 4 (5) (2019) 1158–1163, <https://doi.org/10.1039/C9NH00164F>.
- [17] S. Nanot, E.H. Házor, J.-H. Kim, R.H. Hauge, J. Kono, Optoelectronic properties of single-wall carbon nanotubes, *Adv. Mater.* 24 (36) (2012) 4977–4994, <https://doi.org/10.1002/adma.201201751>.
- [18] J. Garoz-Ruiz, A. Heras, S. Palmero, A. Colina, Development of a Novel Bidimensional Spectroelectrochemistry Cell Using Transfer Single-Walled Carbon Nanotubes Films as Optically Transparent Electrodes, *Anal. Chem.* 87 (12) (2015) 6233–6239, <https://doi.org/10.1021/acs.analchem.5b00923>.
- [19] Z. Yao, C.-C. Zhu, M. Cheng, J. Liu, Mechanical properties of carbon nanotube by molecular dynamics simulation, *Comput. Mater. Sci.* 22 (3–4) (2001) 180–184, [https://doi.org/10.1016/S0927-0256\(01\)00187-2](https://doi.org/10.1016/S0927-0256(01)00187-2).
- [20] J.W. Jo, J.W. Jung, J.U. Lee, W.H. Jo, Fabrication of highly conductive and transparent thin films from single-walled carbon nanotubes using a new non-ionic surfactant via spin coating, *ACS Nano*. 4 (9) (2010) 5382–5388, <https://doi.org/10.1021/nn1009837>.
- [21] M.S. Ata, R. Poon, A.M. Syed, J. Milne, I. Zhitomirsky, New developments in non-covalent surface modification, dispersion and electrophoretic deposition of carbon nanotubes, *Carbon*. 130 (2018) 584–598, <https://doi.org/10.1016/j.carbon.2018.01.066>.
- [22] A. Graf, Y. Zakharko, S.P. Schießl, C. Backes, M. Pföhl, B.S. Flavel, J. Zaumseil, Large scale, selective dispersion of long single-walled carbon nanotubes with high photoluminescence quantum yield by shear force mixing, *Carbon*. 105 (2016) 593–599, <https://doi.org/10.1016/j.carbon.2016.05.002>.
- [23] B. Chandra, A. Afzali, N. Khare, M.M. El-Ashry, G.S. Tulevski, Stable charge-transfer doping of transparent single-walled carbon nanotube films, *Chem. Mater.* 22 (18) (2010) 5179–5183, <https://doi.org/10.1021/cm101085p>.
- [24] Q. Huang, Y. Zhu, Printing Conductive Nanomaterials for Flexible and Stretchable Electronics: A Review of Materials, Processes, and Applications, *Adv. Mater. Technol.* 4 (5) (2019) 1800546, <https://doi.org/10.1002/admt.v4.5.10.1002/admt.201800546>.
- [25] A. Abdelhalim, A. Abdellah, G. Scarpa, P. Lugli, Fabrication of carbon nanotube thin films on flexible substrates by spray deposition and transfer printing, *Carbon*. 61 (2013) 72–79, <https://doi.org/10.1016/j.carbon.2013.04.069>.
- [26] B. Dan, G.C. Irvin, M. Pasquali, Continuous and Scalable Fabrication of Transparent Conducting Carbon Nanotube Films, *ACS Nano*. 3 (4) (2009) 835–843, <https://doi.org/10.1021/nl8008307>.
- [27] H.C. Chen, H.Y. Chiu, K.T. Huang, Raman spectroscopy on 3-D acid-functional single-walled carbon nanotubes for flexible transparent-conducting films deposited with vacuum-filtration and dip-coating, *Diam. Relat. Mater.* 92 (2019) 1–8, <https://doi.org/10.1016/j.diamond.2018.12.002>.
- [28] T. Yang, J. Yang, L. Shi, E. Mäder, Q. Zheng, Highly flexible transparent conductive graphene/single-walled carbon nanotube nanocomposite films produced by Langmuir-Blodgett assembly, *RSC Adv.* 5 (30) (2015) 23650–23657, <https://doi.org/10.1039/C5RA00708A>.
- [29] J.C. Goak, S.H. Lee, J.H. Han, S.H. Jang, K.B. Kim, Y. Seo, Y.-S. Seo, N. Lee, Spectroscopic studies and electrical properties of transparent conductive films fabricated by using surfactant-stabilized single-walled carbon nanotube

- suspensions, *Carbon*. 49 (13) (2011) 4301–4313, <https://doi.org/10.1016/j.carbon.2011.06.007>.
- [30] H.-Z. Geng, D.S. Lee, K.K. Kim, G.H. Han, H.K. Park, Y.H. Lee, Absorption spectroscopy of surfactant-dispersed carbon nanotube film: Modulation of electronic structures, *Chem. Phys. Lett.* 455 (4-6) (2008) 275–278, <https://doi.org/10.1016/j.cplett.2008.02.102>.
- [31] K.A. Shah, B.A. Tali, Synthesis of carbon nanotubes by catalytic chemical vapour deposition: A review on carbon sources, catalysts and substrates, *Mater. Sci. Semicond. Process.* 41 (2016) 67–82, <https://doi.org/10.1016/j.mssp.2015.08.013>.
- [32] V.Y. Iakovlev, D.V. Krasnikov, E.M. Khabushev, J.V. Kolodiaznaia, A. G. Nasibulin, Artificial neural network for predictive synthesis of single-walled carbon nanotubes by aerosol CVD method, *Carbon*. 153 (2019) 100–103, <https://doi.org/10.1016/j.carbon.2019.07.013>.
- [33] K. Yanagi, H. Udoguchi, S. Sagitani, Y. Oshima, T. Takenobu, H. Kataura, T. Ishida, K. Matsuda, Y. Maniwa, Transport mechanisms in metallic and semiconducting single-wall carbon nanotube networks, *ACS Nano*. 4 (7) (2010) 4027–4032, <https://doi.org/10.1021/nn101177n>.
- [34] K.K. Kim, J.J. Bae, H.K. Park, S.M. Kim, H.-Z. Geng, K.A. Park, H.-J. Shin, S.-M. Yoon, A. Benayad, J.-Y. Choi, Y.H. Lee, Fermi level engineering of single-walled carbon nanotubes by AuCl₃ doping, *J. Am. Chem. Soc.* 130 (38) (2008) 12757–12761, <https://doi.org/10.1021/ja8038689>.
- [35] F. Mirri, A.W.K. Ma, T.T. Hsu, N. Behabtu, S.L. Eichmann, C.C. Young, D. E. Tsentelovich, M. Pasquali, High-performance carbon nanotube transparent conductive films by scalable dip coating, *ACS Nano*. 6 (11) (2012) 9737–9744, <https://doi.org/10.1021/nn303201g>.
- [36] D.-W. Shin, J.H. Lee, Y.-H. Kim, S.M. Yu, S.-Y. Park, J.-B. Yoo, A role of HNO₃ on transparent conducting film with single-walled carbon nanotubes, *Nanotechnology*. 20 (47) (2009) 475703, <https://doi.org/10.1088/0957-4484/20/47/475703>.
- [37] K.K. Kim, S.M. Yoon, H.K. Park, H.J. Shin, S.M. Kim, J.J. Bae, Y. Cui, J.M. Kim, J. Y. Choi, Y.H. Lee, Doping strategy of carbon nanotubes with redox chemistry, *New J. Chem.* 34 (2010) 2183–2188, <https://doi.org/10.1039/c0nj00138d>.
- [38] S.M. Kim, K.K. Kim, Y.W. Jo, M.H. Park, S.J. Chae, D.L. Duong, C.W. Yang, J. Kong, Y.h., Lee - Role of anions in the AuCl₃-doping of carbon nanotubes, *ACS Nano*. 5 (2011) 1236–1242, <https://doi.org/10.1021/nn1028532>.
- [39] H.S. Oh, K. Shin, S.J. Lee, D. Shim, J.H. Han, J.M. Myoung, The p-type doping in SWCNT transparent conductive films by spontaneous reduction potential using Ag and Ni, *Chem. Phys. Lett.* 548 (2012) 29–33, <https://doi.org/10.1016/j.cplett.2012.08.005>.
- [40] F. Çolak, Z. Dalkılıç, A. Tabatabaei, R. Atlıbatur, Ü. Çolak, E. Arıc, N. Karatepe, MoOx doped single-walled carbon nanotube films as hole transport layer for organic solar cells, *Acta Phys. Pol. A*. 131 (3) (2017) 474–477.
- [41] S.M. Kim, Y.W. Jo, K.K. Kim, D.L. Duong, H.-J. Shin, J.H. Han, J.-Y. Choi, J. Kong, Y.H. Lee, Transparent Organic P-Dopant in Carbon Nanotubes: Bis (trifluoromethanesulfonyl)imide, *ACS Nano*. 4 (11) (2010) 6998–7004, <https://doi.org/10.1021/nn102175h>.
- [42] Y. Sasaki, H. Okimoto, K. Yoshida, Y. Ono, Y. Iwasa, T. Takenobu, Thermally and environmentally stable carrier doping using a solution method in carbon nanotube films, *Appl. Phys. Express*. 4 (8) (2011) 085102, <https://doi.org/10.1143/APEX.4.085102>.
- [43] E.M. Khabushev, D.V. Krasnikov, O.T. Zaremba, A.P. Tsapenko, A.E. Goldt, A. G. Nasibulin, Machine Learning for Tailoring Optoelectronic Properties of Single-Walled Carbon Nanotube Films, *J. Phys. Chem. Lett.* 10 (21) (2019) 6962–6966, <https://doi.org/10.1021/acs.jpclett.9b02777>.
- [44] A.P. Tsapenko, S.A. Romanov, D.A. Satco, D.V. Krasnikov, P.M. Rajanna, M. Danilson, O. Volobujeva, A.S. Anisimov, A.E. Goldt, A.G. Nasibulin, Aerosol-Assisted Fine-Tuning of Optoelectrical Properties of SWCNT Films, *J. Phys. Chem. Lett.* 10 (14) (2019) 3961–3965, <https://doi.org/10.1021/acs.jpclett.9b01498>.
- [45] A.P. Tsapenko, A.E. Goldt, E. Shulga, Z.I. Popov, K.I. Maslakov, A.S. Anisimov, P. B. Sorokin, A.G. Nasibulin, Highly conductive and transparent films of HAuCl₄-doped single-walled carbon nanotubes for flexible applications, *Carbon*. 130 (2018) 448–457, <https://doi.org/10.1016/j.carbon.2018.01.016>.
- [46] D.S. Montgomery, C.A. Hewitt, R. Barbalace, T. Jones, D.L. Carroll, Spray doping method to create a low-profile high-density carbon nanotube thermoelectric generator, *Carbon*. 96 (2016) 778–781, <https://doi.org/10.1016/j.carbon.2015.09.029>.
- [47] E.Y. Jang, T.J. Kang, H.W. Im, D.W. Kim, Y.H. Kim, Single-walled carbon-nanotube networks on large-area glass substrate by the dip-coating method, *Small*. 4 (12) (2008) 2255–2261, <https://doi.org/10.1002/sml.200800600>.
- [48] P. Kim, T.J. Kang, Large-area fluidic assembly of single-walled carbon nanotubes through dip-coating and directional evaporation, *Micro Nano Syst. Lett.* 5 (1) (2017), <https://doi.org/10.1186/s40486-017-0052-z>.
- [49] M.H. Andrew Ng, L.T. Hartadi, H. Tan, C.H. Patrick Poa, Efficient coating of transparent and conductive carbon nanotube thin films on plastic substrates, *Nanotechnology*. 19 (20) (2008) 205703, <https://doi.org/10.1088/0957-4484/19/20/205703>.
- [50] T. Ackermann, S. Sahakalkan, Y. Zhang, A. Mettenborger, S. Mathur, I. Kolanc, E. Westkamper, Improved performance of transparent silver nanowire electrodes by adding carbon nanotubes, 9th IEEE Int. Conf. Nano/Micro Eng. Mol. Syst. IEEE-NEMS 2014 (2014) 81–85, <https://doi.org/10.1109/NEMS.2014.6908764>.
- [51] G. Xiao, Y.e. Tao, J. Lu, Z. Zhang, Highly conductive and transparent carbon nanotube composite thin films deposited on polyethylene terephthalate solution dipping, *Thin Solid Films*. 518 (10) (2010) 2822–2824, <https://doi.org/10.1016/j.tsf.2009.11.021>.
- [52] M.A. Deshmukh, R. Celiesiute, A. Ramanaviciene, M.D. Shirsat, A. Ramanavicius, EDTA PANI/SWCNTs nanocomposite modified electrode for electrochemical determination of copper (II), lead (II) and mercury (II) ions, *Electrochim. Acta*. 259 (2018) 930–938, <https://doi.org/10.1016/j.electacta.2017.10.131>.
- [53] Y. Tian, M.Y. Timmermans, M. Partanen, A.G. Nasibulin, H. Jiang, Z. Zhu, E. I. Kauppinen, Growth of single-walled carbon nanotubes with controlled diameters and lengths by an aerosol method, *Carbon*. 49 (14) (2011) 4636–4643, <https://doi.org/10.1016/j.carbon.2011.06.036>.
- [54] N.Y. Abu-Thabit, Nanomaterials for flexible transparent conductive films and optoelectronic devices. *Advances in Smart Coatings and Thin Films for Future Industrial and Biomedical Engineering Applications*, Elsevier Inc, 2020, pp. 619–643, <https://doi.org/10.1016/b978-0-12-849870-5.00029-x>.
- [55] D. Satco, A.R.T. Nugraha, M.S. Ukhtary, D. Kopylova, A.G. Nasibulin, R. Saito, Intersubband plasmon excitations in doped carbon nanotubes, *Phys. Rev. B*. 99 (2019), 075403, <https://doi.org/10.1103/PhysRevB.99.075403>.
- [56] S. Li, J.G. Park, R. Liang, C. Zhang, B. Wang, Effects of solvent immersion and evaporation on the electrical conductance of pre-stressed carbon nanotube buckypapers, *Nanotechnology*. 22 (36) (2011) 365706, <https://doi.org/10.1088/0957-4484/22/36/365706>.
- [57] D. Grosso, How to exploit the full potential of the dip-coating process to better control film formation, *J. Mater. Chem.* 21 (2011) 17033–17038, <https://doi.org/10.1039/c1jm12837j>.
- [58] X. Liang, Z. jun Wang, C. jun Liu, Size-Controlled Synthesis of Colloidal Gold Nanoparticles at Room Temperature Under the Influence of Glow Discharge, *Nanoscale Res. Lett.* 5 (2010) 124 – 129, doi: 10.1007/s11671-009-9453-0.